

Surface modification of silica nanoparticles: a new strategy for the realization of self-organized fluorescence chemosensors†

Enrico Rampazzo,^a Elena Brasola,^a Silvia Marcuz,^a Fabrizio Mancin,^a Paolo Tecilla^{*b} and Umberto Tonellato^{*a}

Received 8th February 2005, Accepted 18th April 2005

First published as an Advance Article on the web 5th May 2005

DOI: 10.1039/b502052b

The self-organization of the proper subunits of a fluorescence chemosensor on the surface of silica nanoparticles allows the easy design and realization of new effective sensing systems. Commercially available silica particles (20 nm diameter) were functionalized with triethoxysilane derivatives of selective Cu(II) ligands and fluorescent dyes. Grafting of the sensor components to the particle surface ensures the spatial proximity between the sensor components and, as a consequence, binding of Cu(II) ions by the ligand subunits leads to quenching of the fluorescent units emission. In 9 : 1 DMSO–water solution, the coated silica nanoparticles (CSNs) selectively detect copper ions down to nanomolar concentrations. The operative range of the sensors can be tuned either by switching the ligand units or by modification of the components ratio. Sensors with the desired photophysical properties can be easily prepared by using different fluorescent dyes. Moreover, the organization of the network of sensor components gives rise to cooperative and collective effects: on one hand, the ligand subunits bound to the particle surfaces cooperate to form multivalent binding sites with an increased affinity for the Cu(II) ions; on the other hand, binding of a single metal ion leads to the quenching of several fluorescent groups producing a remarkable signal amplification.

Introduction

The interest in fluorescence chemosensors, *i.e.* molecular systems that recognize and signal the presence of a selected substrate by a variation of their fluorescence emission, is continuously growing.¹ In fact, such systems provide a sensitive and selective method to evaluate the presence and the concentration of different substrates. In addition, their molecular dimensions allow high response rate and spatial resolution in the analyte detection, also making possible intracellular monitoring of selected species in medical and biochemical studies.

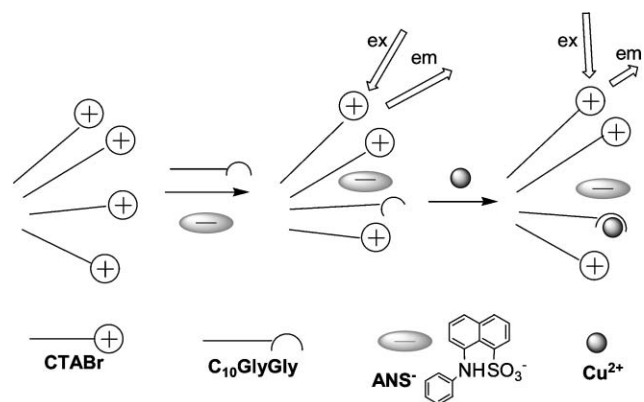
In their typical design, fluorescent chemosensors are molecules composed by one or more substrate binding units and photoactive components, which generate the fluorescence signal.¹ The chemical complexity of such systems varies greatly from case to case, as the sensor components can be integrated, complementing each other, or simply connected by spacers. However, the synthetic efforts involved in the realization and in the subsequent optimization of chemosensors may be demanding.

Self-assembling and self-organizing methodologies have attracted increasing attention during recent years in the chemistry of complex systems with functional properties. Indeed, they are at the basis of the so-called “bottom-up” approach, as the building of complex structures with this

strategy simply requires the design and synthesis of a limited number of relatively simple building blocks which are then allowed to self-organize spontaneously.² As a result of the molecular organization into a supramolecular assembly, novel properties and functions may result and lead to possible important applications.

In view of that, exploiting the self-organization of receptors and fluorescent dyes may, at least partially, allow the synthetic problems connected to classical systems to be overcome and provide an efficient strategy for the easy realization and optimization of fluorescence chemosensors.

A few years ago, we reported a novel methodology to self-assemble a fluorescent chemosensor for Cu(II) ions within surfactant aggregates.³ The system (Scheme 1) was based on

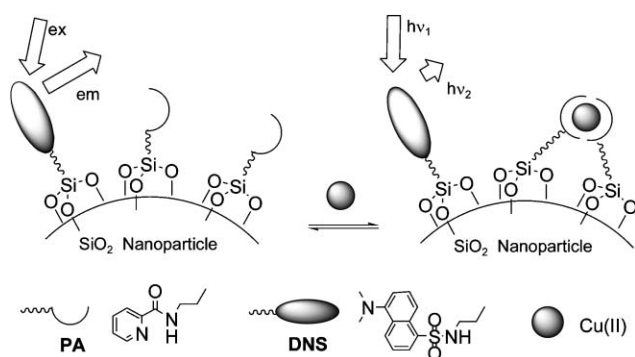


Scheme 1 Surfactant aggregate based self-organized fluorescence chemosensors.

† Electronic supplementary information (ESI) available: synthesis of compounds 1–8; potentiometric titrations; quenching amplification. See <http://www.rsc.org/suppdata/jm/b5/b502052b/>
*tecilla@dsch.univ.trieste.it (Paolo Tecilla)
umberto.tonellato@unipd.it (Umberto Tonellato)

co-micelles made by a lipophilic dipeptide ligand (*N*-decylglycylglycine), a fluorescent dye (8-anilinaphthalensulfonic acid, ANS) and a cationic surfactant (hexadecyltrimethylammonium bromide, CTABr). The concentration of the species within the micellar aggregate ensured the spatial proximity between the ligand and the dye so that the complexation of the Cu(II) ions by the glycylglycine moiety resulted in a signal generated by the quenching of the dye fluorescence emission. This self-assembled chemosensor allowed Cu(II) concentrations to be determined down to the micromolar range in water at pH 7. The main advantages of such a system are: a) selectivity, mainly due to the ligand choice; b) simplicity: the sole mixing of the components (two of them, CTABr and ANS, are commercially available) in water was required to realize the sensor; c) modularity, which allowed the modification or the optimization of the system by simply substituting one of the components; d) the possibility to tune the detection range just by the modification of the components ratio.^{3,4} Then, analogous strategies, based on Langmuir–Blodgett films⁵ and trialkoxysilane self-assembled monolayers on quartz surfaces,⁶ were successfully explored.⁷ However, the actual applicability of such systems is limited by several factors. In particular, surfactant aggregates are delicate objects due to their dynamic nature: they form only above the critical micellar concentration, the fraction of non-micellized components may be not negligible, and they are very sensitive to environmental conditions, such as temperature and ionic strength, which can affect the reproducibility of the sensor response.

To overcome such limitations, in a recent communication⁸ we described a strategy for the realization of self-organized fluorescence chemosensors for Cu(II) ions obtained by surface modification of silica nanoparticles. Commercially available particles (20 nm diameter) were functionalized (Scheme 2) with the triethoxysilane derivatives of the selective Cu(II) ligand picolinamide (**1a**, Chart 1) and the fluorophore dansylamide (**3a**, Chart 1). As in the case of surfactant-based systems, grafting of the sensor components to the particle surface ensures the spatial proximity required to signal Cu(II) by quenching of the fluorescence emission. In 9 : 1 DMSO–water solution, the coated silica nanoparticles (CSNs) selectively detect copper ions down to micromolar concentrations and the operating range of the sensor can be tuned by the simple



Scheme 2 Coated silica nanoparticles based self-organized fluorescence chemosensors.

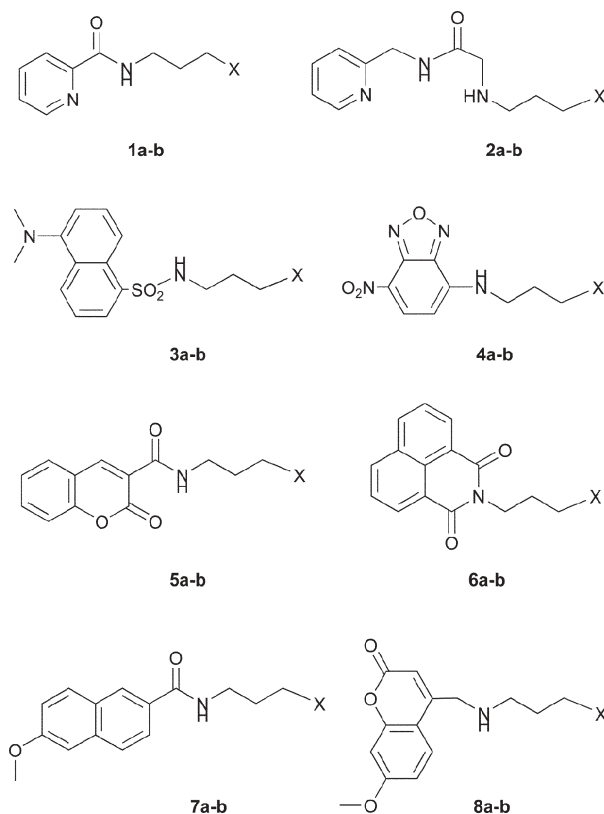


Chart 1 Ligands and fluorescent dyes (a: X = Si(OEt)₃; b: X = H).

modification of the components ratio. Moreover, cooperation of the ligand subunits bound to the particles surfaces to form binding sites with an increased affinity for the substrate (Scheme 2) was demonstrated.

Indeed, modification of nanoparticle surfaces offers an attractive approach to the realization of non-dynamic organized assemblies of functional subunits which would not suffer from the limitations of surfactant-based systems.⁹ Silica nanoparticles, in particular, are suitable for the realization of fluorescence chemosensors: they are transparent to light, photophysically inert and their surface can be easily modified by reaction with alkoxy silane derivatives.¹⁰

The use of polymer nanoparticles as chemically inert matrices to entrap fluorescent chemosensors for intracellular applications has been proposed by the groups of Kopelman and Rosenzweig.¹¹ The nanoparticle matrix not only protects the sensor from interference with the cellular content, but also allows the realization of multicomponent systems. Montalti and coworkers investigated fluorophore functionalized silica nanoparticles and reported evidence that collective processes can arise from the organization of the components in an extended network.¹⁰ In a recent report, Larpent and coworkers described a study on latex nanoparticles containing a Cyclam ligand and a BODIPY fluorescent dye: they found significant signal amplification in Cu(II) detection due to the quenching of 44 fluorophores by a single metal ion.¹²

In this paper, we highlight the potentiality of this strategy for the realization of self-organized fluorescence chemosensors, showing that a library of sensor subunits can be easily realized and used to prepare different sensing systems

with the most suitable features for the desired application. New collective effects due to the spatial proximity of a great number of subunits, which can give rise to an improvement of the sensor performance, have been recognized and will be described.¹³

Results and discussion

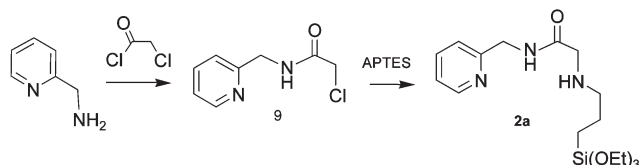
Design, synthesis and characterization

The Cu(II) selective ligands and fluorescent dyes designed for the present study are shown in Chart 1. Alkoxysilane derivatives **1a–8a**, needed for silica nanoparticle functionalization, were prepared. The corresponding compounds not bearing the triethoxysilane moiety (**1b–8b**) were also synthesized for comparison purposes.

The choice of receptors **1** and **2** was based on the scrutiny of several Cu(II) selective ligands, usually based on aminoamides or dipeptides, reported in the literature.¹⁴ The key recognition motif of such ligands is the presence of an amidic group in a central position. As a matter of fact, the interaction between the deprotonated amidic group and Cu(II) ions is particularly strong and such a unique property ensures that, at neutral pH conditions, Cu(II) is the only metal ion capable of strongly binding to amide based ligands by promoting their deprotonation. Other transition metals show little or no affinity at all for the same ligands, unless much more basic conditions are used. Based on these premises, we selected picolinamide (**1**) and (2-pyridinmethyl)-glycinamide (**2**) as Cu(II) selective recognition elements for our sensors. The presence, when possible, of the pyridine group instead of more widely employed alkyl amines implies several advantages: i) no protection of the amino group is required during the synthesis of the ligand, ii) the chromatographic purification of the alkoxysilane derivatives is made easier due to the increased lipophilicity and a lesser basicity, iii) the solubility in organic solvents is improved.

Picolinamide is reported¹⁵ to be a selective ligand for Cu(II) at neutral pH. Ligand **2** was newly designed, in order to further increase the Cu(II) affinity of the sensor recognition units, by adding a third chelating site. Binding constants were evaluated by potentiometric titrations in water (see ESI†). In the case of ligand **1b**, precipitation of Cu(OH)₂ prevented the titration of solutions containing equimolar amounts of ligand and metal ion. Experiments performed with a 3-fold excess of **1b** over Cu(NO₃)₂ revealed the formation of complexes with both 1 : 2 and 1 : 3 metal to ligand stoichiometry, and the log *K_n* values ($K_n = [ML_n]/[H^+]^n/[LH]^n \cdot [M]$, see ref. 16) were respectively –8.6 and –17.6. In the case of ligand **2b**, titration of an equimolar solution of ligand and metal yield a log *K₁* value of 3.3 for the 1 : 1 complex. Apparent binding constants at a fixed pH value ($K_n(\text{app}) = [ML_n]/[LH]^n \cdot [M]$) allow an easier comparison of the binding strength of the ligands: at pH 7, log *K₂*(app) = 5.4 and log *K₃*(app) = 3.4 for **1b** and log *K₁*(app) = 10.3 for **2b**.¹⁶

The synthetic route for the alkoxysilane derivatives **1a–8a** and the model compounds **1b–8b** was straightforward. With the exception of ligands **2** and fluorophores **6**, the synthesis of the desired compounds just required a one-step condensation of a properly activated derivative with commercially available



Scheme 3

3-aminopropyl-triethoxysilane (APTES) or propylamine. Fluorescent derivatives **3**, **4** and **8** were directly prepared from commercially available dansyl chloride, NBD chloride (4-chloro-7-nitrobenzofurazan) and 4-bromomethyl-7-methoxycoumarin, while ligand **1** and fluorophores **5** and **7** were prepared respectively from picolinic acid, coumarin-3-carboxylic acid and 6-methoxynaphthalen-2-carboxylic acid *via* thionyl chloride activation.

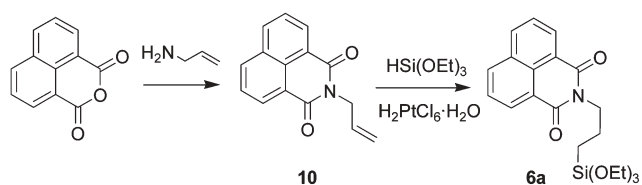
A two-step synthesis (Scheme 3) was required for ligands **2**: picolinamide was reacted with 2-chloroacetyl chloride to yield the corresponding amide **9** which was then condensed with APTES or propylamine.

In the case of the fluorophore derivatives **6** an alternative synthetic route not requiring APTES was followed (Scheme 4). 1,8-Naphthalic anhydride was condensed with 3-aminopropene to yield the corresponding imide **10**, which was then reacted with triethoxysilane in the presence of hydrogen hexachloroplatinate to obtain **6a**.

In any case, purification of the triethoxysilane derivatives was accomplished using flash chromatography on silica gel.

Coated silica nanoparticles (CSNs) were prepared from the triethoxy derivatives **1a–8a** following the procedure recently reported by Montalti and coworkers.⁹ Commercially available LUDOX silica nanoparticles were heated at 70 °C in a 1 : 1 : 1 mixture of water, ethanol and acetic acid in the presence of the desired coating subunits. Subsequent purification involved precipitation, extraction in organic solvent and size exclusion chromatography.

CNS characterized by different ligand to dye ratios, hereafter defined by the ligand molar fraction χ , were prepared using ligands **1a** and **2a** and fluorophore **3a** simply by modulation of the concentration of the alkoxysilane derivatives in the reaction mixture. In the case of ligand **1a** (and dye **3a**) the composition of the coating was always found to be close to that of the reaction mixture, while using ligand **2a**, a substantially more abundant dye fraction than that of the reaction mixture was observed in the resulting CSNs. This is likely to be ascribed to the fact that the secondary amine of ligand **2a** is protonated in the acidic reaction medium, at variance with the weakly basic pyridine and aniline nitrogens of ligand **1a** and fluorophore **3a**. Hence, electrostatic repulsion between the positively charged ligand **2a** subunits may disfavor



Scheme 4

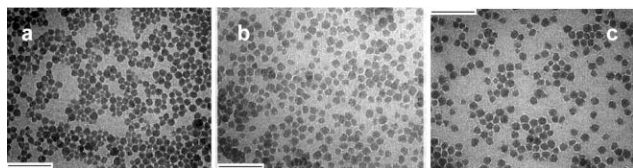


Fig. 1 TEM images of LUDOX silica nanoparticles (a), CSNs with ligand **1a** and dye **3a** (b, $\chi = 0.5$), CSNs with ligand **2a** and dye **3a** (c, $\chi = 0.25$). The bars correspond to 100 nm.

the attachment to the nanoparticle surface in favor of the dye subunit.

Nanoparticles covered by the sole fluorescent subunits **4a–8a** turned out to be not dispersible in any solvent and only mixed coated nanoparticles with an excess of ligand **1a** were prepared from these compounds.

The resulting particles were investigated by transmission electron microscopy (TEM, Fig. 1). Uncoated LUDOX silica particles show a mean diameter of 15 ± 6 nm, while CSNs have diameters which range from about 16 ± 5 nm, when functionalized with mixtures containing ligand **1a**, to 18 ± 6 nm in the case of ligand **2a**. These results indicate, particularly in the case of CNS coated with ligand **2a**, that the growth of a multilayer thin film of the organic silane precursors on the surface of the LUDOX silica nanoparticles is more likely than a monolayer coating. The possibility of self-condensation of the silane derivatives in the acidic reaction conditions, leading to the formation of nanoparticles lacking the LUDOX silica core, was investigated by carrying out the coating reaction in the absence of the LUDOX nanoparticles. TEM analysis of the reaction product revealed the absence of any recognizable nanoparticles.

The coated silica nanoparticles can be stored as dry powders and are dispersible in non-polar organic solvents (CHCl_3 , CH_2Cl_2) and in DMSO containing water up to 10%. UV-Vis and fluorescence spectra of the fluorophores immobilized on the silica nanoparticles are similar to those of the reference dyes **3b–8b**. ^1H NMR analysis showed the signal broadening typical of immobilized subunits on the nanoparticle surfaces and, in most cases, allowed the determination of the ratio of the components present in the coating.

The number of components present on a single nanoparticle can be roughly estimated^{10,17} on the basis of four parameters: the dye and the ligand concentration in the CSNs solutions (determined by absorbance and NMR measured component ratio), the particle radii and the density of LUDOX silica.¹⁸ In our case such estimation gives an average of 7000 subunits per particle, similar to that calculated by Montalti and coworkers for **1a** coated CSNs.¹⁰ In the approximation of a single monolayer of subunits on a smooth sphere, this value would correspond to an average distance between two subunits of about 4 Å.

Cu(II) sensing

The effect of the addition of an aqueous $\text{Cu}(\text{NO}_3)_2$ solution on the fluorescence emission of CSNs solutions (10% water–DMSO, CSNs $0.0015 \text{ mg mL}^{-1}$, HEPES buffer 0.01 M, pH 7.0) coated respectively by **3a** alone, **1a** and **3a** ($\chi = 0.5$), **2a**

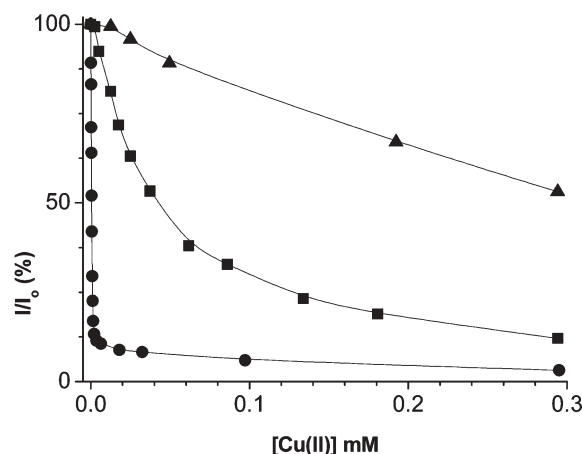


Fig. 2 Spectrofluorimetric titration of CSNs ($0.0015 \text{ mg mL}^{-1}$) with $\text{Cu}(\text{NO}_3)_2$ in 10% water–DMSO, HEPES buffer 0.01 M pH 7, 25 °C, $\lambda_{\text{exc}} = 340 \text{ nm}$, $\lambda_{\text{em}} = 520 \text{ nm}$ (▲: CNSs coated by only **3a**; ■: CNSs coated by **1a** and **3a**, $\chi = 0.5$; ●: CNSs coated by **2a** and **3a**, $\chi = 0.5$).

and **3a** ($\chi = 0.5$), is reported in Fig. 2. In each case, on increasing the metal ion concentration, the fluorescence emission decreases. The effect is quite modest in the case of nanoparticles coated by **3a** alone, while almost complete quenching (down to about 5% of the initial value) is reached for the CSNs coated with ligands **1a** and **2a**. The systems are stable and reproducible and different titration experiments gave identical results within the experimental error (<2%).

The observed fluorescence quenching is the result of the binding of the $\text{Cu}(\text{II})$ ions to the nanoparticles. This is supported by the saturation behavior of the profiles reported in Fig. 2, diagnostic of non-collisional quenching, and by the fact that the emission recovers its initial value after the addition of an excess of EDTA, a strongly competitive ligand. As a consequence, the sensitivity of CSNs containing **2a** is much higher than that of the nanoparticles containing **1a**, which is a weaker ligand for $\text{Cu}(\text{II})$. Fig. 2 indicates also that CSNs coated with **3a** alone show a fluorescence decrease upon $\text{Cu}(\text{II})$ addition (Fig. 2, ▲). A similar effect is obtained by adding $\text{Cu}(\text{II})$ to a **3b** solution indicating that, in this solvent system, the dansylamide unit alone can provide weak $\text{Cu}(\text{II})$ binding sites. However, the presence of the ligand subunits is necessary to achieve a strong binding of the substrate and authenticate the CSNs as sensors.

As highlighted in Fig. 2, the sensitivity gain obtained by using ligand **2a** is excellent: if the amount of $\text{Cu}(\text{II})$ necessary to decrease the initial fluorescence emission by 10% ($[\text{Cu}(\text{II})]_{10\%}$) is taken as the detection limit, such a limiting $\text{Cu}(\text{II})$ concentration decreases from $6.8 \times 10^{-6} \text{ M}$ to $3.0 \times 10^{-8} \text{ M}$ on going from **1a** to **2a** containing CSNs.

The sensitivity of the CNS to $\text{Cu}(\text{II})$ is notably related to the concentration of the nanoparticles. Fig. 3 shows the dependence of the $[\text{Cu}(\text{II})]_{10\%}$ values on the amount of **2a/3a** CSNs present in the solution: the sensitivity improves by decreasing the nanoparticle concentration to reach, between 0.0015 and $0.0006 \text{ mg mL}^{-1}$, a limiting value close to 30 nM. Further dilution of the CSNs leads to a worsening of sensitivity. A similar trend is observed also in the case of **1a/3a** nanoparticles, but the benefits deriving from CSNs dilution are

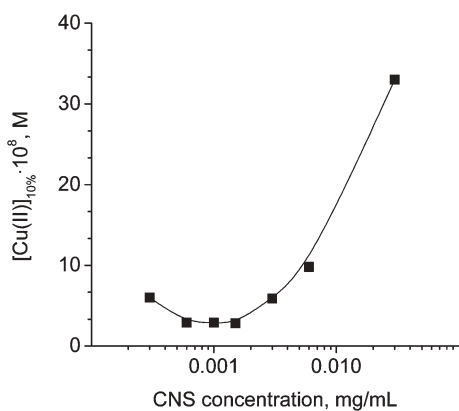


Fig. 3 $[\text{Cu(II)}]_{10\%}$ values for CSNs coated by **2a** and **3a** ($\chi = 0.5$) as a function of the total particle concentration. Conditions: 10% water–DMSO, HEPES buffer 0.01 M pH 7, 25 °C, $\lambda_{\text{exc}} = 340$ nm, $\lambda_{\text{em}} = 520$ nm.

much less important. Such behavior can be explained as the result of two opposite effects: on one hand, by decreasing the nanoparticle concentration the amount of Cu(II) ions necessary to quench the emission of all the fluorophores is reduced and, hence, the sensitivity is improved; on the other hand, the decrease of the ligand concentration leads to a decrease of the overall Cu(II) binding ability of the nanoparticles and to a lower sensitivity. With the strong ligand **2a** the positive effect of dilution prevails down to very low nanoparticle concentrations while, in the case of the weaker ligand **1a**, the two effects almost cancel each other over a large concentration range.

The ratio between the ligand and the dye in the CNSs coating, *i.e.* the χ value, is another relevant factor that allows the tuning of the sensor sensitivity. Fig. 4 shows the variation of the fluorescence emission upon addition of Cu(II) to different solutions containing nanoparticles coated by **2a/3a** (Fig. 4a) and by **1a/3a** (Fig. 4b) in different ligand to fluorescent ratios. In both cases the increase of the χ value, *i.e.* the increase of the ligand content of the CNSs coating, leads to an improvement of the sensitivity. In the case of **2a/3a** CNSs, the quenching profiles show a clear biphasic behavior: first, the strong quenching of part of the initial fluorescence emission is observed at low Cu(II) concentrations; subsequently, further addition of Cu(II) produces a minor emission decrease which still reaches a plateau value at about 5% of the initial emission for very high Cu(II) concentrations. Interestingly, **2a/3a** CNSs with different χ values display a similar Cu(II) affinity at low metal ion concentrations, differing only in the amount of fluorescence quenching produced. The extent of the initial emission decrease is roughly proportional to the amount of ligand subunit present in the nanoparticles and reaches complete quenching for $\chi = 0.5$. Further increments of the amount of ligand in the CNSs coating do not produce any sensitivity improvement.

As already observed in the previous experiments, the **1a/3a** CNSs are generally less sensitive to Cu(II) than **2a/3a** CNSs, probably due to the minor affinity of these particles for the metal ion. In addition, in the case of the **1a/3a** CNSs the sensitivity variation spans over a larger χ interval, and levels off only when the amount of ligand subunits in the coating

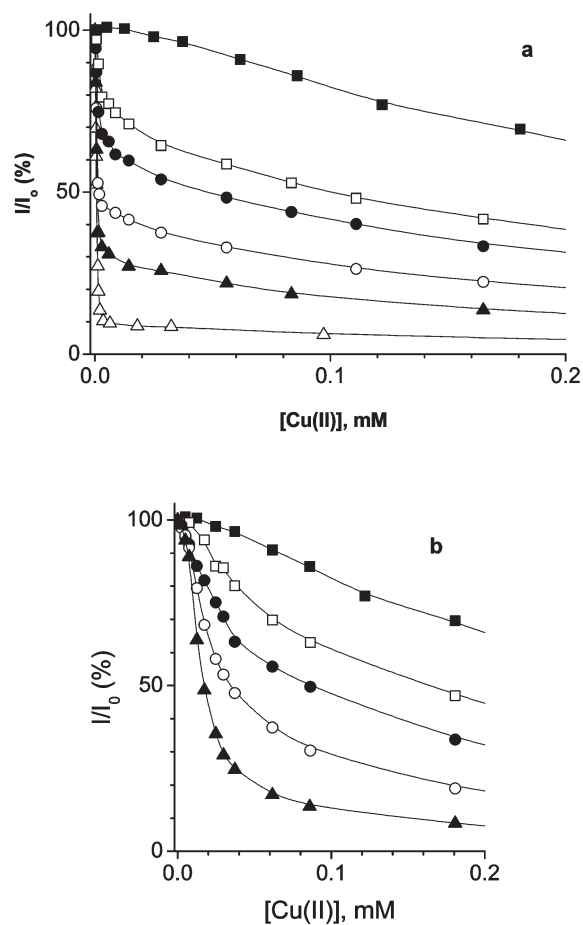


Fig. 4 Spectrofluorimetric titration of: a) **2a/3a** CNSs (0.003 mg mL^{-1}) with $\text{Cu(NO}_3)_2$ (■: $\chi = 0$; □: $\chi = 0.02$; ●: $\chi = 0.04$; ○: $\chi = 0.07$; ▲: $\chi = 0.26$; △: $\chi = 0.50$); b) **1a/3a** CNSs (0.003 mg mL^{-1}) with $\text{Cu(NO}_3)_2$ (■: $\chi = 0$; □: $\chi = 0.15$; ●: $\chi = 0.4$; ○: $\chi = 0.55$; ▲: $\chi = 0.81$). Conditions: 10% water–DMSO, HEPES buffer 0.01 M pH 7, 25 °C, $\lambda_{\text{exc}} = 340$ nm, $\lambda_{\text{em}} = 520$ nm. The lines represent the fit of the data (see text).

reaches about 70%. With these CNSs, however, the biphasic behavior of the quenching profiles is less evident and different Cu(II) affinity is shown by CNSs with different χ values.

The different behavior of the two CNSs series is the result of the different Cu(II) binding ability of the ligands subunits **1a** and **2a**. In the case of the stronger Cu(II) chelator **2a**, complexation of the metal ions by the ligand subunits occurs at much lower concentration than the binding to the dansyl subunits. The two processes are hence well distinguishable in the titration profile. In the first part, the Cu(II) ions are presumably complexed by the ligand subunits on the nanoparticle surface and quench the fluorescence emission of the surrounding dansyl groups. Once all the ligand subunits have been saturated by Cu(II) ions, the CNSs show a residual emission that is probably due to those dye subunits which are not close enough to a binding site to interact with the metal ion. Further addition of Cu(II) causes the quenching of this residual emission due to the low affinity interaction of the dansyl units themselves with the metal ions, as observed in the case of the CNSs coated by **3a** only (Fig. 2). In the case of **2a/3a** CNSs, containing only 2% of ligand subunits, the extent

of the initial quenching is about 20% (Fig. 4a). This value suggests that a single Cu(II) ion bound to a **2a** subunit can quench the emission of about 10 surrounding dyes.

This hypothesis is supported by interpolation of the titration profiles. A simplified model involving the presence of two independent and different binding sites for metal ions with 1 : 1 stoichiometry was used. The interpolation of each profile reported in Fig. 4a gave a good fit and average $\log K_{\text{app}}$ values of 6.1 and 3.7 were determined respectively for the **2a** and **3a** subunits. A $\log K$ value of 3.5 was obtained by the fit of the titration profile obtained for CSNs coated with **3a** alone. Thus, using these apparent binding constants, it is possible to calculate the metal ion content of the nanoparticles. In the case of **2a/3a** CSNs containing a 2% of ligand subunits (0.003 mg mL^{-1} , $[\mathbf{2a}]_{\text{tot}} = 8.9 \times 10^{-8} \text{ M}$, $[\mathbf{3a}]_{\text{tot}} = 4.4 \times 10^{-6} \text{ M}$), the presence of a Cu(II) concentration of $1.0 \times 10^{-6} \text{ M}$ causes a 10.3% quenching of the initial fluorescence emission. The amount of metal ions bound to the particles in these conditions is $4.73 \times 10^{-8} \text{ M}$: hence, each Cu(II) ion causes the quenching of about 9.5 dansyl subunits.

As 20% of the dansyl subunits are quenched in the 2% ligand containing CSNs, a quenching radius of about 0.7 nm can be estimated for a single Cu(II) ion.¹⁹ With the CSNs containing 4%, 7% and 26% of ligand subunit the initial quenching increases respectively to 35%, 55% and 70%, and reaches 100% for a ligand content of 50%. Of course, as the ligand content of the coating increases, the number of dye units surrounding each ligand decreases and the “spheres of influence” of the different binding sites overlap reducing the number of dyes effectively quenched by a single Cu(II) ion. When ligand content reaches $\chi = 0.5$ all the fluorescent groups are close enough to a binding site to interact with it and by consequence no benefit is obtained by further increments of the χ value.

In the case of CSNs containing the weaker ligand **1a**, the biphasic shape of the titration profiles is much less evident and, most noticeably, the Cu(II) affinity of the nanoparticles apparently increases with increasing χ values. The ligand strength is quite modest and binding of Cu(II) ions occurs almost simultaneously both at **1a** and **3a** subunits. In fact, fitting of the titration profiles for **1a/3a** with a χ value of 0.15 gave $\log K$ values respectively of 3.86 and 3.1. At a constant nanoparticle concentration, the increase of the χ value implies an increase of the total ligand concentration in the solution and, as a consequence, a larger extent of binding of the metal ions. However, also in this case, cooperative effects have been shown to play an important role. This was highlighted by the results of experiments carried out on nanoparticle solutions with different χ values but with a constant overall concentration of ligand **1a**.⁸ These results indicated that CSNs with large χ have an intrinsic greater affinity for the metal ion and this can reasonably be ascribed to the surface-organization of the ligand subunits. At low χ values, the picolinamide groups are far from each other on the particle surface and operate as individual ligands. As the χ value increases, also the relative density of binding units on the CSNs surface increases and this may lead to the formation of multivalent binding sites (e.g. with 2 : 1 or 3 : 1 ligand to metal stoichiometries) with a greater Cu(II) affinity, as shown in Scheme 2.

The easy interchange of the sensor component is one of the major advantages of the self-assembling strategies. The results so far reported show how it is possible to switch the ligand subunit of the CSNs in order to modulate the sensor operative range. By the same means, the signaling unit, *i.e.* the fluorescent dye, can also be easily changed to set up a series of nanoparticle-based sensors with different photophysical features. CSNs coated by **1a** and all the trialkoxysilane dye derivatives **3a–8a** have been prepared. As highlighted by Fig. 5b, the emission spectra of these CSNs span over a large wavelength interval from 300 to 600 nm (correspondingly, excitation wavelengths range from 285 to 466 nm), allowing the choice of the more suitable sensor for the desired application. Titration (Fig. 5a) of the different nanoparticles with Cu(II) shows almost identical behaviour for all the CSNs, confirming that the recognition of the metal ion by the sensor is due essentially to its interaction with the binding subunit.

Then, we turned our attention to selectivity, which is the main feature to validate the CSNs as sensors. The effect of the addition of other divalent metal ions, such as Ca(II), Mg(II), Zn(II), Cd(II), Co(II), Ni(II), Fe(II) and Pb(II), was evaluated in

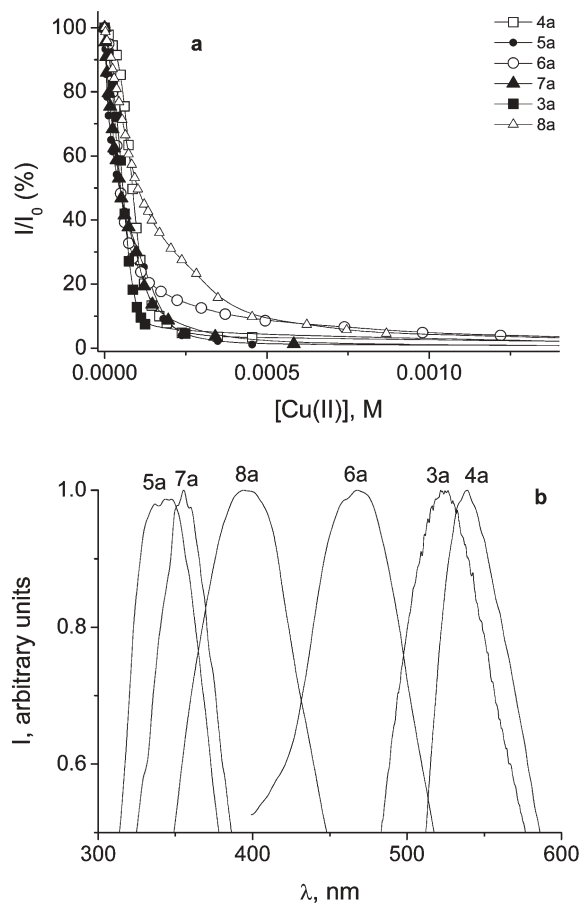


Fig. 5 Spectrofluorimetric titration with Cu(NO₃)₂ (a) and normalized emission spectra (b) of CSNs coated by **1a** and dyes **3a–8a** ($\chi = 0.90$, 0.003 mg mL^{-1} , \blacksquare : **3a**, $\lambda_{\text{exc}} = 340 \text{ nm}$, $\lambda_{\text{em}} = 520 \text{ nm}$; \square : **4a**, $\lambda_{\text{exc}} = 466 \text{ nm}$, $\lambda_{\text{em}} = 538 \text{ nm}$; \bullet : **5a**, $\lambda_{\text{exc}} = 295 \text{ nm}$, $\lambda_{\text{em}} = 345 \text{ nm}$; \circ : **6a**, $\lambda_{\text{exc}} = 333 \text{ nm}$, $\lambda_{\text{em}} = 470 \text{ nm}$; \blacktriangle : **7a**, $\lambda_{\text{exc}} = 285 \text{ nm}$, $\lambda_{\text{em}} = 357 \text{ nm}$; \triangle : **8a**, $\lambda_{\text{exc}} = 322 \text{ nm}$, $\lambda_{\text{em}} = 394 \text{ nm}$). Conditions: 10% water–DMSO, HEPES buffer 0.01 M pH 7, 25 °C.

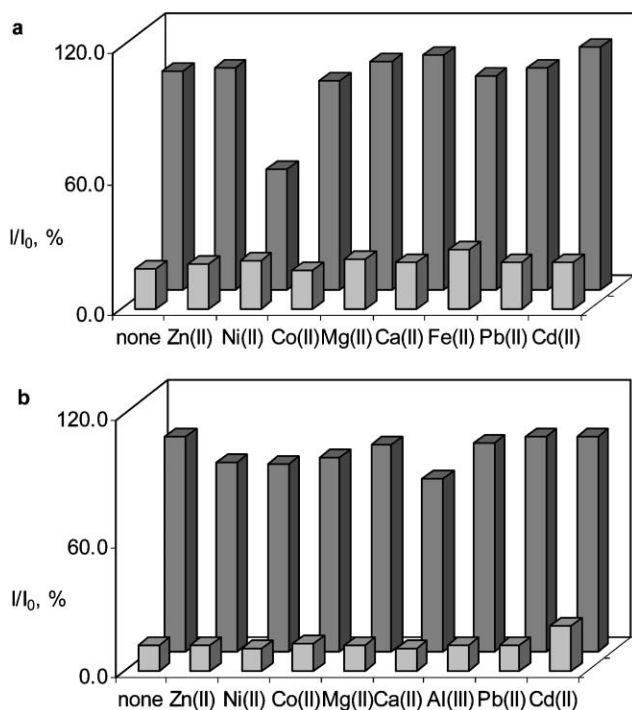


Fig. 6 Relative fluorescence intensity of: a) **1a/3a** ($\chi = 0.86$, 0.003 mg mL^{-1}) CSNs in the presence of the indicated metal ions alone ($50 \mu\text{M}$, back row) and with Cu(II) ($50 \mu\text{M}$, front row); b) **2a/3a** ($\chi = 0.50$, $0.0015 \text{ mg mL}^{-1}$) CSNs in the presence of the indicated metal ions alone ($2.5 \mu\text{M}$, back row) and with Cu(II) ($2.5 \mu\text{M}$, front row). Conditions: 10% water–DMSO, HEPES buffer 0.01 M pH 7, $25 \text{ }^\circ\text{C}$, $\lambda_{\text{exc}} = 340 \text{ nm}$, $\lambda_{\text{em}} = 520 \text{ nm}$.

the competition experiments reported in Figs. 6 and 7. In the case of **1a/3a** CSNs, with $\chi = 0.86$ (Fig. 6a), the presence of $50 \mu\text{M}$ of Cu(II) quenches the emission of CSNs to 20% of the initial value, while the presence of the same concentration of the other cations does not produce any effect on the fluorescence of the CSNs, with the exception of Ni(II) which brings about a 45% decrease of the emission. This result is in line with the reported ability of picolinamide ligand to bind

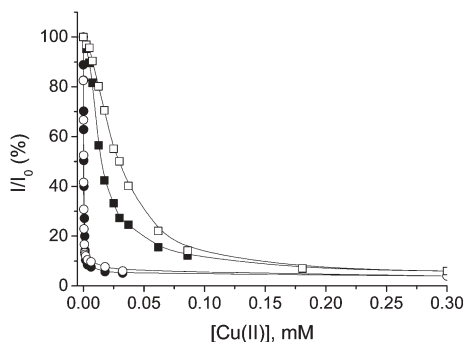


Fig. 7 Spectrofluorimetric titration of **1a/3a** (squares, $\chi = 0.86$, 0.003 mg mL^{-1}) and **2a/3a** (circles, $\chi = 0.50$, $0.0015 \text{ mg mL}^{-1}$) CSNs with $\text{Cu}(\text{NO}_3)_2$ in the absence (filled symbols) and in the presence (empty symbols) of CaCl_2 , MgCl_2 , $\text{Zn}(\text{NO}_3)_2$, $\text{Cd}(\text{NO}_3)_2$, CoCl_2 , $\text{Ni}(\text{NO}_3)_2$, $\text{Fe}(\text{NO}_3)_2$ and $\text{Pb}(\text{NO}_3)_2$ each $50 \mu\text{M}$ (in the case of **1a/3a** CSNs) or $25 \mu\text{M}$ (in the case of **2a/3a** CSNs). Conditions: 10% water–DMSO, HEPES buffer 0.01 M pH 7, $25 \text{ }^\circ\text{C}$, $\lambda_{\text{exc}} = 340 \text{ nm}$, $\lambda_{\text{em}} = 520 \text{ nm}$.

Cu(II) with a very large affinity and Ni(II) ions with a much lower one.¹⁴ In fact, after the addition of Cu(II) ($50 \mu\text{M}$) to the solutions containing each other metal ion, the emission is reduced to the same value (20%) observed with Cu(II) alone, thus showing that there is no interference due to these ions in the Cu(II) determination. Moreover, titration with Cu(II) of a solution containing the CSNs and all the above metal ions, each at a $50 \mu\text{M}$ concentration, results in a quenching profile very similar to that obtained in the absence of any interferent (Fig. 7, squares).

CSNs coated with **2a** and **3a** ($\chi = 0.5$), at lower metal ion concentrations, behave in a very similar way, showing an even better selectivity toward Ni(II) (Fig. 6b). In fact, while the emission of the CSNs is almost completely quenched (88% decrease) in the presence of $2.5 \mu\text{M}$ of Cu(II), the same amount of Ni(II) ions produced no (or moderate, up to 10%) emission decrease. Again, competitive titration with Cu(II) of a solution containing the CSNs and all the above metal ions (each $25 \mu\text{M}$) results in a quenching profile identical to that obtained in the absence of any interferent (Fig. 7, circles). Such results underline the fact that the CSNs respond selectively to Cu(II) ions even in the presence of an excess of several other divalent metal ions. Using these CSNs, however, remarkable fluorescence quenching is observed at higher concentrations of metal ion: in the presence of a $50 \mu\text{M}$ concentration of Ni(II) the emission is reduced to 50%, and the same amount of Co(II), Ca(II) and Zn(II) induces a 30% emission decrease. Further investigation is needed to explain such effects, although it is likely that the presence of several neighboring secondary amino groups bound to the **2a** ligand subunits may lead to the formation of non-specific metal ion binding sites on the nanoparticle surfaces.

Conclusions

Although Cu(II) sensing does not attract great interest by itself, as numerous analytic methods are already available for this metal ion, the results presented in this work highlight the potential of the use of coated silica nanoparticles in the realization of self-assembled fluorescence chemosensors for transition metal ions and, in future developments, for other substrates. When compared to the sensors in the surfactant aggregates, the CSNs based systems retain most of their peculiar advantages. High sensitivity, down to the nanomolar range in the case of the **2a/3a** nanoparticles, and excellent selectivity are obtained. Realization of the sensor just requires the mixing of the selected components in the reaction vessel and, unlike the micellar systems, a short work-up. Tuning of the operating range can be obtained by the simple modification of the components ratio. Optimization or modification of the sensor features can be obtained by simply changing one of the coating components for a different one.

In addition, CSNs based sensors present several new advantages. Particularly noteworthy is the possibility to store the sensor as a dry powder, to simply prepare and calibrate batch solutions and, as a consequence, achieve a much better reproducibility than the “on demand” prepared micellar systems. Furthermore, due to their non-dynamic nature, CSNs are not sensitive to environmental conditions, such as

the composition of the medium in which the analysis is carried out, in contrast with the case of surfactant aggregates

Besides all these important advantages, the possibility of cooperative effects due to the grafting of the sensor components to the nanoparticle surface is to be duly emphasized. In the case of **1a/3a** nanoparticles, cooperation between the ligand subunits was previously shown to lead to the formation of Cu(II) binding sites with a greater metal ion affinity. Moreover, in the case of **2a/3a** CSNs here reported, the binding of a single Cu(II) ion apparently quenches the emission of about ten surrounding dansyl dyes. This gives rise to a signal amplification which contributes, along with the high Cu(II) affinity of the **2a** ligand, to the achievement of the remarkable sensitivity of these CSNs. Similar collective phenomena have been observed in dansyl functionalized dendrimers,²⁰ in dansyl coated silica nanoparticles¹⁰ and in fluorescent dyes impregnated polymer nanoparticles.¹² These observations indicate that the role of the nanoparticle scaffold is more subtle than merely keeping close the sensor components: the spatial proximity and organization of the coating components can eventually lead to the tuning or modification of the intrinsic properties of the insulated subunits.

Of course, there are still some limitations of this approach to be addressed. The first one is related to the synthesis of the derivatives required for the nanoparticle surface functionalization. Handling the trialkoxysilane derivatives is more ticklish than that of the lipophilic derivatives required for micellar sensors and not all the sensor components, which can be designed, are easily synthesized. However, due also to the growing interest in materials science and nanotechnology, several trialkoxysilane derivatives, such as **3a**, are already commercially available and many others, predictably soon, will be put on the market. Once the library of the available and feasible components is defined, the possible combination and opportunities to realize diverse systems will become easier and stimulating.

A more delicate problem involves the solubility of the CSNs. The solvent system employed in this study, 10% water–DMSO, is suitable for chemical analysis, as Cu(II) water solutions can be added directly to the CSNs solution, but it is, of course, not suitable for more desirable applications of such nanosensors, as in the case of intracellular analysis. Moreover, water solubility would allow more practical nanoparticle purification methods such as dialysis or ultrafiltration. A possible solution to this limitation could be, as reported for Au nanoparticles,²¹ the addition of a third component to the coating, such as poly(ethylene glycol) derivatives, capable of improving the water solubility of the CSNs. Finally, extension of this strategy to substrates that do not intrinsically quench fluorescence emission as Cu(II) or Ni(II) is to be addressed.

Work is in progress in our laboratories to better define the scope, the application and, possibly, overcome the limitations of this strategy.

Experimental

General

All commercially available solvents and reagents were used as received without further purification. TLC analyses were

performed using Merck 60 F₂₅₄ (0.25 mm) precoated silica gel glass plates and Machery-Nagel Poligram SIL G/UV₂₅₄ precoated plastic sheets (0.25 mm). Preparative column chromatography was carried out on glass columns packed with Macherey-Nagel 60 (70–230 mesh) and on Kieselgel 60, 0.063 mm Merck silica gel.

NMR spectra were recorded with a Bruker AC 250F spectrometer. Chemical shifts are reported relative to tetramethylsilane as internal standard. Signals in NMR spectra are reported as follows: s = singlet; d = doublet, t = triplet, q = quartet, m = multiplet, b = broadened. ESI-MS mass spectra were obtained with a Navigator ThermoQuest-Finnigan mass spectrometer. GC-MS analyses were performed on an Agilent 6850 Series GC System, equipped with a quadrupole mass analyzer and with a fused silica capillary column EC-1 Alltech (stationary phase polymethylsiloxane, length 30 m, internal diameter 0.25 mm and film thickness 0.25 μm). Generally, unless otherwise specified a 250 °C injector temperature was used.

Elemental analyses were performed by the Laboratorio di Microanalisi of the Department of Chemical Sciences of the University of Padova. Transmission Electron Microscopy (TEM) experiments were performed at the CSPA of the University of Trieste. TEM images of the particles were obtained with a Philips EM 208 transmission electron microscope operating at 100 KeV. Samples for TEM were prepared by spreading a drop of nanoparticles solution in CHCl₃ (~5 mg mL⁻¹) onto standard carbon-coated copper grids (200 mesh). Dimensional analysis of nanoparticles from TEM images was made with the Image J software, developed by the Research Services Branch (RSB) of National Institute of Mental Health (NIMH), USA (<http://rsb.info.nih.gov/nih-image/about.html>).

Potentiometric titrations were performed using a Metrohm 716 DMS Titrino dynamic titrator. UV-VIS absorption measurements were performed at 25 °C by means of Perkin-Elmer Lambda 16 e 45 spectrophotometers equipped with thermostated cell holders. Quartz cells with optical pathlength of 1 cm were used. Fluorescence spectra were recorded at 25 °C with a LS-50B spectrofluorimeter equipped with a Hamamatsu R928 photomultiplier and thermostated cell holder, quartz cells with optical pathlength of 1 cm were used.

The synthetic procedures for compounds **1–8** are reported in the ESI.†

Potentiometric titrations

Protonation constants and Cu(II) complex formation constants for ligands **1b** and **2b** were determined by pH potentiometric titrations (25 °C, 0.10 M NaCl). Solutions approximately 1 × 10⁻³ M of the hydrochloride salts of the ligands and, when necessary, Cu(NO₃)₂ were titrated using a 0.1 M sodium hydroxide solution. The electrode system was calibrated by titrating a 0.01 M solution of HCl so that the pK_w value was 13.78. The pH and the volume of added NaOH data were fitted with the computer program BEST²² to obtain the desired protonation and complex formation constants.

Spectrophotometric titrations

Cu(NO₃)₂, Zn(NO₃)₂, Ni(NO₃)₂, CoCl₂, Fe(NO₃)₂, CdCl₂, Pb(NO₃)₂, CaCl₂ and MgCl₂ were analytical grade products. Metal ion stock solutions were titrated against EDTA following standard procedures. Solution used during the spectrophotometric measurements and titrations were prepared using deionized water ($R > 18 \text{ M}\Omega$), obtained with a Milli-Q (Millipore) purification system, or HPLC grade dimethylsulfoxide. The buffer 4-(2-hydroxyethyl)-1-piperazineethanesulfonic acid (HEPES, Alrich) was used as received and stock solutions (0.2 M) were prepared using Milli-Q water.

Stock solutions of CSNs were prepared in HPLC grade CHCl₃. The total molar concentration of **3a** subunits was determined from the absorbance at 340 nm using the ϵ value ($4650 \pm 30 \text{ M}^{-1} \text{ cm}^{-1}$) of *N*-propyl-dansylamide. The total concentration of **1a** and **2a** subunits was calculated using the coating components ratio determined by ¹H-NMR spectroscopy. The desired amount of CHCl₃ solution was then transferred into a volumetric flask, the solvent was evaporated under a gentle N₂ stream and the CSNs were redissolved in DMSO (90%) and water (10%) buffered at pH 7.0 (HEPES, 0.01 M). 2 mL aliquots of these solutions were transferred into fluorescence quartz cells, small volumes (up to 50 μL) of concentrated metal ions solutions were added and the fluorescence or absorption spectra were recorded.

Fitting of the titration curves was performed with the software package Scientist 2.01.²³ A model involving the formation of 1 : 1 complexes of Cu(II) with two different ligands was used. Total concentrations of ligand and dye subunits, as determined by UV-Vis absorbance and NMR ratios, were set as invariable parameters. Errors on the fits were always less than 10%.

Preparation of coated silica nanoparticles

Preparation of CSNs **1a/3a** with $\chi = 0.50$ is reported as an example of a general procedure. All the other CSNs were prepared following the same procedure with different amounts of the precursors **1a–8a** (the total amount of the two alkoxy silane derivatives was fixed at 0.25 mmol). The effective relative amount of the precursors on the surface of the CSNs was determined by ¹H-NMR spectroscopy.

Preparation of **1a/3a** CSNs ($c = 0.5$)

1a (42 mg, 0.13 mmol) and 54 mg (0.13 mmol) of **3a** were placed in a round bottom flask and then dissolved with 1.25 mL of ethanol, 1.25 mL of water and 1.25 mL of acetic acid. A water suspension (125 μL) of silica nanoparticles (LUDOX AS-30 Colloidal Silica, Aldrich) was added. The reaction mixture was warmed at 80 °C under stirring for 48 hours. After this time ethanol was evaporated under reduced pressure and solid NaHCO₃ was added to the suspension to reach a pH value between 7 and 8. The precipitate was filtered and washed with a borate buffer solution (pH 9.5, 5 \times 2 mL) and with water (5 \times 2 mL). The solid was dried under vacuum and redissolved with 100 mL of dichloromethane. The organic solution was washed with water (100 mL) and dried over Na₂SO₄. The crude solid material

obtained after the evaporation of the solvent was finally purified by gel permeation chromatography (Sephadex LH20, CH₂Cl₂). For this batch a χ value of 0.50 was determined by ¹H-NMR analysis.

1a/3a CSNs (precursor ratio 1 : 1)

¹H-NMR (250 MHz, CDCl₃, 25 °C) δ : 0.67 (4H, NCH₂CH₂CH₂-Si, **1a** and **3a**); 1.70 (4H, NCH₂CH₂CH₂-Si, **1a** and **3a**); 2.86 (8H, NCH₂CH₂CH₂-Si and N(CH₃)₂, **3a**); 3.42 (2H, NCH₂CH₂CH₂-Si, **1a**); 6.19 (1H, very broad, NHCH₂CH₂CH₂-Si, **3a**); 7.12, 7.38 (3H, CH(DNS) and CH(py)); 7.79 (1H, CH(Py)); 8.22, 8.39, 8.48 (7H, NHCH₂CH₂CH₂-Si and *H*_{arom}, **1a** and **3a**). FT-IR (KBr): 3370 (OH); 2928, 2869 (CH); 1666 (C=O); 1523 (HNCO); 1304 (S=O); 1112 (Si–O) cm⁻¹.

2a/3a CSNs (precursor ratio 1 : 1)

¹H-NMR (250 MHz, CDCl₃, 25 °C) δ : 0.59 (4H, NCH₂CH₂CH₂-Si, **2a** and **3a**); 1.60 (4H, NCH₂CH₂CH₂-Si, **2a** and **3a**); 2.64 (2H, NCH₂CH₂CH₂-Si, **2a**; this signal is strongly overlapped with the next); 2.85 (8H, NCH₂CH₂CH₂-Si and N(CH₃)₂, **3a**); 3.36 (2H, (CO)CH₂NH, **2a**); 4.54 ((CO)NHCH₂-(pyr), **2a**); 6.2 (1H, very broad, NHCH₂CH₂CH₂-Si, **3a**); 7.10, 7.44, 8.18, 8.34, 8.46 (11 H *H*_{arom} and (CO)NHCH₂-(pyr) **2a** and **3a**).

1a/4a CSNs (precursor ratio 10 : 1)

¹H-NMR (250 MHz, CDCl₃, 25 °C) δ : 0.70(NCH₂CH₂CH₂-Si, **1a** and **4a**); 1.72 (NCH₂CH₂CH₂-Si, **1a** and **4a**); 3.42 (NCH₂CH₂CH₂-Si, **1a** and **4a**); 6.16, 7.37, 7.80, 8.19, 8.48 (7H, *H*_{arom} and NHCH₂CH₂CH₂-Si, **1a** and **4a**).

1a/5a CSNs (precursor ratio 10 : 1)

¹H-NMR (250 MHz, CDCl₃, 25 °C) δ : 0.72 (NCH₂CH₂CH₂-Si, **1a** and **5a**); 1.75 (NCH₂CH₂CH₂-Si, **1a** and **5a**); 3.44 (NCH₂CH₂CH₂-Si, **1a** and **5a**); 7.36, 7.61, 7.82, 8.21, 8.48, 8.82 (*H*_{arom} and NHCH₂CH₂CH₂-Si, **1a** and **5a**).

1a/6a CSNs (precursor ratio 10 : 1)

¹H-NMR (250 MHz, CDCl₃, 25 °C) δ : 0.72(NCH₂CH₂CH₂-Si, **1a** and **6a**); 1.74 (NCH₂CH₂CH₂-Si, **1a** and **6a**); 3.42 (NCH₂CH₂CH₂-Si, **1a**); 4.10 (NCH₂CH₂CH₂-Si, **6a**); 7.35, 7.78, 8.14, 8.47 (*H*_{arom} and NHCH₂CH₂CH₂-Si, **1a** and **6a**).

1a/7a CSNs (precursor ratio 10 : 1)

¹H-NMR (250 MHz, CDCl₃, 25 °C) δ : 0.72(NCH₂CH₂CH₂-Si, **1a** and **7a**); 1.74 (NCH₂CH₂CH₂-Si, **1a** and **7a**); 3.44 (NCH₂CH₂CH₂-Si, **1a** and **7a**); 3.90 (OCH₃, **7a**); 7.07, 7.36, 7.78, 8.20, 8.47 (*H*_{arom} and NHCH₂CH₂CH₂-Si, **1a** and **7a**).

1a/8a CSNs (precursor ratio 10 : 1)

¹H-NMR (250 MHz, CDCl₃, 25 °C) δ : 0.71(NCH₂CH₂CH₂-Si, **1a** and **8a**); 1.72 (NCH₂CH₂CH₂-Si, **1a** and **8a**); 3.41 (NCH₂CH₂CH₂-Si, **1a**); 4.25 (OCH₃ and NHCH₂-arom, **8a**); 7.33, 7.75, 8.16, 8.46 (*H*_{arom} and NHCH₂CH₂CH₂-Si, **1a** and **8a**).

Acknowledgements

The authors thank Mr. Claudio Gamboz and Prof. Maria Rosa Soranzo (CSPA, University of Trieste), for kind help with TEM analysis. Financial support for this research has been partly provided by the Ministry of Instruction, University and Research (MIUR contracts 2003030309 and 2003037580) and by University of Padova (University Research Project CPDA034893).

Enrico Rampazzo,^a Elena Brasola,^a Silvia Marcuz,^a Fabrizio Mancin,^a Paolo Tecilla^{*b} and Umberto Tonellato^{*a}

^aDipartimento di Chimica Organica and Istituto CNR di Tecnologia delle Membrane - Sezione di Padova, Università di Padova, via Marzolo 1, I-35131, Padova, Italy. E-mail: umberto.tonellato@unipd.it; Fax: +39 0498275239; Tel: +39 0498275269

^bDipartimento di Scienze Chimiche, Università di Trieste, via Giorgieri 1, I-34127, Italy. E-mail: tecilla@dsch.univ.trieste.it; Fax: +39 0405583903; Tel: +39 0405583925

References

- (a) Special Issue on "Luminescent Sensors", ed. L. Fabbrizzi, *Coord. Chem. Rev.*, 2000, **205**; (b) A. P. de Silva, H. Q. N. Gunaratne, T. Gunnlaugsson, A. J. M. Huxley, C. P. McCoy, J. T. Rademacher and T. E. Rice, *Chem. Rev.*, 1997, **97**, 1515–1566; (c) *Fluorescent Chemosensors for Ion and Molecule Recognition*, ed. A. W. Czarnik, ACS Symposium Series 538, American Chemical Society, Washington DC, 1993.
- (a) S. Mann, *Chem. Commun.*, 2004, 1–4; (b) S. Hecht, *Angew. Chem., Int. Ed.*, 2003, **42**, 24–26.
- (a) P. Grandini, F. Mancin, P. Tecilla, P. Scrimin and U. Tonellato, *Angew. Chem., Int. Ed.*, 1999, **38**, 3061–3064; (b) M. Berton, F. Mancin, G. Stocchero, P. Tecilla and U. Tonellato, *Langmuir*, 2001, **17**, 7521–7528.
- Other examples of the same approach have been recently reported: (a) Y. Diaz-Fernandez, A. Perez-Gramatges, V. Amendola, F. Foti, C. Mangano, P. Pallavicini and S. Patroni, *Chem. Commun.*, 2004, 1650–1651; (b) Y. Diaz-Fernandez, A. Perez-Gramatges, S. Rodriguez-Calvo, C. Mangano and P. Pallavicini, *Chem. Phys. Lett.*, 2004, **398**, 245–249.
- Y. Zheng, J. Orbulescu, X. Ji, F. M. Andreopoulos, S. M. Pham and R. M. Leblanc, *J. Am. Chem. Soc.*, 2003, **125**, 2680–2686.
- (a) M. Crego-Calama and D. N. Reinhoudt, *Adv. Mater.*, 2001, **13**, 1171–1174; (b) L. Basabe-Desmonts, J. Beld, R. S. Zimmerman, J. Hernando, P. Mela, M. F. Garcia Parajo, N. F. van Hulst, A. van den Berg, D. N. Reinhoudt and M. Crego-Calama, *J. Am. Chem. Soc.*, 2004, **126**, 7293–7299.
- An alternative approach to the realization of self-assembled chemosensors, called "chemosensing ensemble", has been proposed and involves the displacement of a non-covalent dye-receptor complex by the substrate. See for example: (a) S. L. Wiskur, H. Ait-Haddou, J. J. Lavigne and E. V. Anslyn, *Acc. Chem. Res.*, 2001, **34**, 963–972; (b) M. A. Hortalà, L. Fabbrizzi, N. Marcotte, F. Stomeo and A. Taglietti, *J. Am. Chem. Soc.*, 2003, **125**, 20–21.
- E. Brasola, F. Mancin, E. Rampazzo, P. Tecilla and U. Tonellato, *Chem. Commun.*, 2003, 3026–3027.
- Selected reviews: (a) R. Shenhar and V. M. Rotello, *Acc. Chem. Res.*, 2003, **36**, 549–561; (b) C. M. Niemeyer, *Angew. Chem., Int. Ed.*, 2001, **40**, 4128–4158.
- M. Montalti, L. Prodi, N. Zaccheroni and G. Falini, *J. Am. Chem. Soc.*, 2002, **124**, 13540–13546.
- (a) S. M. Buck, Y. E. L. Koo, E. Park, H. Xu, M. Brasuel, M. A. Philbert and R. Kopelman, *Curr. Opin. Chem. Biol.*, 2004, **8**, 540–546; (b) S. M. Buck, H. Xu, M. Brasuel, M. A. Philbert and R. Kopelman, *Talanta*, 2004, **63**, 41–59; (c) J. Lu and Z. Rosenzweig, *Fresenius J. Anal. Chem.*, 2000, **366**, 569–575.
- R. Méallet-Renault, R. Pansu, S. Amigoni-Gerbierb and C. Larpent, *Chem. Commun.*, 2004, 2344–2345.
- Other examples of nanoparticles based self-organized fluorescence sensors have been recently reported: (a) K. M. Gáttas-Asfura and R. M. Leblanc, *Chem. Commun.*, 2003, 2684–2685; (b) Y. Chen and Z. Rosenzweig, *Anal. Chem.*, 2002, **74**, 5132–5138.
- H. Siegel and R. B. Martin, *Chem. Rev.*, 1982, **82**, 385–426.
- H. L. Conley and R. B. Martin, *J. Phys. Chem.*, 1965, **69**, 2914–2923.
- Complex formation involves deprotonation of amide nitrogen: the overall binding constant is hence: $K_n = [ML_n] \cdot [H^+]^n / [LH]^n \cdot [M]$, where M is the metal ion and LH the neutral ligand.
- N. M. Okun, T. M. Anderson and C. L. Hill, *J. Am. Chem. Soc.*, 2003, **125**, 3194–3195.
- A. van Blaaderen and A. P. M. Kentgens, *J. Non-Cryst. Solids*, 1992, **149**, 161–178.
- In the hypothesis of a homogeneous distribution of the subunits, the quenching of 20% of the dyes implies that 20% of the particle surface area is the quenching "dominion" of the Cu(II) ions. A single particle (radius 9 nm) contains about 7000 subunits and hence 140 ligand units.
- F. Vogtle, S. Gesteremann, C. Kauffmann, P. Ceroni, V. Vicinelli and V. Balzani, *J. Am. Chem. Soc.*, 2000, **122**, 10398–10404.
- P. Pengo, S. Polizzi, M. Battagliarin, L. Pasquato and P. Scrimin, *J. Mater. Chem.*, 2003, **13**, 2471–2478.
- A. E. Martell and R. J. Motekaitis, *Determination and Use of Stability Constants*, 2nd edn., VCH, New York, 1992.
- Scientist 2.01, Micromath Scientific Software, Salt Lake City, 1995.